Simplified measurement of point spread functions of hyperspectral cameras for assessment of spatial coregistration

Torbjørn Skauli, Hans Erling Torkildsen

Torbjørn Skauli, Hans Erling Torkildsen, "Simplified measurement of point spread functions of hyperspectral cameras for assessment of spatial coregistration," Proc. SPIE 10986, Algorithms, Technologies, and Applications for Multispectral and Hyperspectral Imagery XXV, 109860E (14 May 2019); doi: 10.1117/12.2520219

SPIE.

Event: SPIE Defense + Commercial Sensing, 2019, Baltimore, Maryland, United States

Simplified measurement of point spread functions of hyperspectral cameras for assessment of spatial coregistration

Torbjørn Skauli*, Hans Erling Torkildsen
Norwegian Defence Research Establishment (FFI)
P O Box 25, 2027 Kjeller, Norway

ABSTRACT

In multi- and hyperspectral imaging, spatial coregistration of the point spread functions (PSFs) of all bands within each pixel is critical for the integrity of measured spectra. There is a need to define a standardized method for characterizing coregistration error. We propose a method that estimates PSFs from the product of line spread functions (LSFs) recorded in two orthogonal directions. Coregistration is then evaluated according to the PSF difference metric [T. Skauli, Opt. Expr. vol. 20, p. 918 (2012)]. Experimental results on two pushbroom hyperspectral cameras show good correspondence with measurements based on the full PSF, provided that LSF scan directions are aligned with axes of symmetry in the optics. Even a maximally unfavourable choice of scan directions gives meaningful estimates of coregistration error. The proposed method may have potential as a standard for coregistration characterization.

Keywords: Hyperspectral imaging, Multispectral imaging, Remote sensing, Optical design, Coregistration, Modulation transfer function

1. INTRODUCTION

Multi- and hyperspectral imaging techniques are being used in an increasing range of applications, leading to a growing community of users. New spectral imaging technologies and products are being developed to meet application needs. It is increasingly important for camera developers and vendors to specify the performance of their products to users in an adequate and unified way. It has been recognized that the current state of the art of specifying spectral cameras has some shortcomings, not least since the long established methods used to characterize conventional cameras do not cover all aspects of spectral imaging performance. This shortfall has led to an initiative to standardize hyperspectral cameras, organized under the IEEE P4001 working group [1].

One of the characteristics that are unique to spectral imaging is the degree of spatial coregistration between different spectral bands in each pixel. It is clearly desirable that for a given pixel, all bands record light from the scene or object with the same distribution of sensitivity, as described by the point spread function (PSF). The left part of Figure 1 illustrates that with a homogeneous scene, coregistration error has no effect on the measured spectrum. It is therefore possible to perform accurate radiometric calibration of a spectral camera by using a uniform calibration source such as an integrating sphere. However, the accuracy of such radiometric calibration does not represent the possible distortion of measured pixel spectra due to spatial coregistration errors. Band-to-band differences in PSF position or shape may introduce significant artifacts in the measured spectra if the scene is heterogeneous within the area seen by a pixel, as illustrated in the right part of Figure 1. In practical cases, spectral cameras are often used for imaging of scenes with subpixel heterogeneity, for example a vegetated sunlit scene with shadows of all sizes, where coregistration errors may lead to spectral artifacts much stronger than the noise level of the camera. Therefore, a measure of coregistration error is needed as part of a specification of a spectral camera.

In this paper we briefly review different ways to characterize coregistration that have been discussed during the work of the P4001 group. We then propose a combination of measurement and analysis which may be an interesting candidate for inclusion in a future standard.

Algorithms, Technologies, and Applications for Multispectral and Hyperspectral Imagery XXV,
edited by Miguel Velez-Reyes, David W. Messinger, Proc. of SPIE Vol. 10986, 109860E

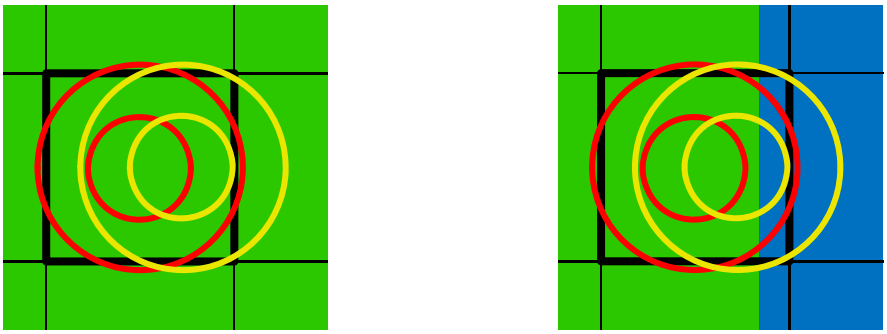

Figure 1. Effect of coregistration error. The figure illustrates a pixel in a nominal pixel grid (black) and contours of the pixel PSF for two bands (red and yellow). The camera has a "keystone" coregistration error in the form of an offset of the yellow band. On the left, the scene is uniform (green) and the signals in the two bands give a correct representation of the scene spectrum. On the right, the scene contains two different materials (green and blue) which both contribute to the signals in each band. In this case, the weighting of the scene materials is different for the two bands, and the recorded spectrum violates the normal assumption of linear mixing within the pixel.

2. BRIEF REVIEW OF COREGISTRATION CHARACTERIZATION METHODS

Coregistration has most often been characterized by "keystone error", the relative PSF peak position offset between bands illustrated in Figure 1. This conventional measure of coregistration is insensitive to differences in PSF shape. In cases where the PSF shape is well behaved, a simple measure of offset may be sufficient to represent coregistration performance. However, it is well known that PSFs may have more complex shapes that vary from band to band, as illustrated in by the experimental results in Figure 5 below.

A common way to assess PSF shape difference is through measures of PSF width. The full width at half maximum (FWHM) is a conventional measure of peak width which has often been applied to characterization of hyperspectral camera PSFs. The peak width and position together can give a good measure of coregistration error in cases where the optics is well behaved [2]. The FWHM is an incomplete description of PSF shape, however, and does not define a bound on the fraction of the PSF energy contained within the FWHM. Therefore, significant differences may exist between the PSFs of two bands, even if their peak position and FWHM are the same. Some improvement is brought by the method used in [3], where peak width is defined to enclose a fraction of the PSF equivalent to the integral between the half-maximum points of a Gaussian. Still, this leaves 24% of the PSF energy outside the defined width.

A further improvement can be brought by the method proposed in [4], which measures the difference between PSFs, either the maximum or the standard deviation, within the pixel area. In this method, the pixel area is defined as the region where the mean PSF over all bands is larger than that of the neighboring pixels. This method is therefore sensitive to differences in the PSF shape from one band to another within the pixel area. As defined, the maximum misregistration according to the method of [4] will tend to give a good measure of coregistration error for point sources such as stars. For the more common case of extended sources, it must be noted that even the method of [4] will disregard some fraction of PSF energy, namely the fraction that spills into neighboring pixels. This can be a significant fraction of the PSF, not least since new image sensors offer ever smaller pixels, so that the detector pixel pitch may be comparable to, or even smaller than, the PSF width.

The measures of coregistration mentioned above are in their basic form defined in one spatial dimension, while the PSF represents a distribution of sensitivity over the two spatial dimensions of the image. One-dimensional measures of coregistration are normally applied to the readily measurable line spread function (LSF) which is a projection of the PSF. (In [4] it is specified that a point source is used, which instead will measure a section through the PSF.) As illustrated in Figure 2, the shape of a measured LSF may depend strongly on the scanning direction. Such loss of information is inherent in any method based on 1D scanning of the PSF. For line-scanning "pushbroom" camera architectures, it is natural to apply the one-dimensional measures separately in the along-track and across-track directions, such as in [2]. If desired, an overall figure of merit for coregistration can then be derived, for example from the mean or maximum of the one-dimensional measures.

An alternative two-dimensional measure of coregistration was proposed in [5] and independently in [6]. This method quantifies the coregistration error between two bands as the integrated difference between their normalized PSFs

according to (1) below. In [7] it is shown that this method characterizes the maximum possible spectral error in the case where the scene is a heterogeneous mixture of extended sources, as illustrated in Figures 1 and 2. This error metric will here be referred to as the "PSF difference metric" (PDM). For instrument specification, a favorable mathematical property of the PDM is that it gives an exact upper bound on the spectral error that may occur in the common case of a scene composed of extended sources, without making any further assumptions about the scene.

Figure 2. Illustration of the need for two-dimensional measurement of the PSF shape in order to fully characterize coregistration. The contours illustrate PSFs of two bands in the same pixel, with coregistration errors that may be difficult to capture based on measurement of LSF. The PSFs are overlaid on a heterogeneous scene to illustrate the corresponding unequal spatial sampling. Left: A pair of PSFs which will appear to be equal when judged by an LSF measured in the vertical direction. Right: A pair of PSFs which will tend to have nearly equal LSFs measured in both horizontal and vertical directions. Thus a characterization of coregistration from a 1D scan may fail to detect the coregistration error in these cases. This paper explores the use of approximate PSFs formed by multiplying LSFs recorded in two orthogonal directions. The figure on the right illustrates that this method will have some limitations.

A practical disadvantage of the PDM method is that it requires measurement of the full two-dimensional PSF, as outlined in [7]. In [8,9], it was shown that such imaging of the PSF is feasible, by tomographic reconstruction from line scans. It is probably also possible to measure the PSF more directly by raster scanning of a point source, though possibly with some practical challenges related to the brightness and stability of the source. In any case, a two-dimensional imaging of the PSF inevitably requires a more complex measurement setup, and a longer measuring time, compared to methods based on measurement of LSF in one or two directions. It may therefore be undesirable to include a full mapping of the PSF as part of a standard for hyperspectral camera characterization.

In this paper, we explore the feasibility of characterizing coregistration by applying the PDM to approximate PSFs formed as the product of two LSFs recorded in orthogonal directions. This holds the promise of using the mathematically favorable PDM to estimate coregistration error, while using the same simple measurement procedures as for other coregistration characterization methods.

3. DEFINITION OF AN APPROXIMATE PDM METHOD

Let $f_i(x,y)$ be the point spread function of band i in a pixel under study. To be precise, $f_i(x,y)$ is the spatial distribution of camera responsivity within a particular pixel and band, and includes effects of the optics, the image sensor detector element, any scanning movement, and any resampling or other preprocessing. (In [7] this is denoted the sampling point spread function, SPSF.) The PSF is normalized to unit integral:

$$\iint_{x,y} f(x,y)\,dxdy = 1$$

(The band index i will be dropped where it is not needed.) The basic PDM is defined for a pair of bands i and j as

$$\varepsilon_{ij} = \frac{1}{2}\iint_{x,y} \left| f_j(x,y) - f_i(x,y) \right| dxdy \qquad (1)$$

The integral in (1) is the volume between PSFs, as illustrated in Figure 3. Thus for identical PSFs, $\varepsilon_{ij} = 0$ and for completely disjoint PSFs, $\varepsilon_{ij} = 1$. A camera with many bands can be characterized by the mean or maximum of ε_{ij} over all band pairs, as discussed in [7].

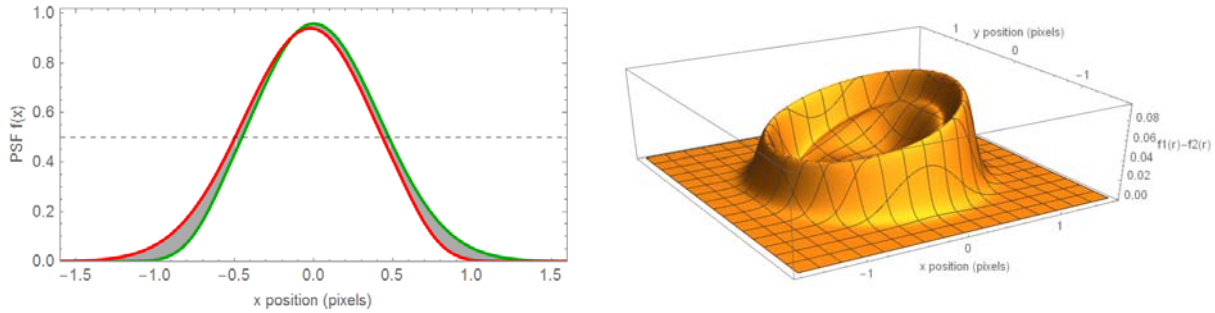

Figure 3. Illustration of the PSF difference metric (PDM) and the significance of the tails of the PSF. Left: A 1D section through the PSF for two bands (green and red) with a small difference in peak width and a small offset in the x direction. The gray region is a 1D illustration of the integrand in the PSF difference metric (1). Right: a 2D plot of the integrand in (1) if the two PSFs are assumed to be rotationally symmetric about the pixel center, illustrating the larger area represented by the PSF tails.

When considering the different methods for coregistration characterization, a somewhat subtle point is that a 1D representation of PSF and coregistration may underestimate the significance of the tails of the PSF. Consider the illustrative case in Figure 3 where two bands have Gaussian PSFs with slight differences between them. In the 1D section through the PSF, the region outside the half-max points contains about 24% of the energy. In 2D, however, the tails of the PSF outside the half-max contour contribute about half of the total energy. The difference between PSFs in the integrand of the PDM (1) is weighted up accordingly, as illustrated in the right part of the figure. In general, the effect of band-to-band differences in the tails of the PSF will tend to be weighted up by the radius from the pixel center.

Consider measurement of two line spread functions by scanning a line source over the PSF in the x and y directions. Neglecting noise and measurement error, the resulting observed line spread functions are

$$LSFx(x) = \int_y f(x,y)dy \quad \text{and} \quad LSFy(y) = \int_x f(x,y)dx$$

Observe that these LSFs will have unit integral. The correct scaling of a measured LSF can thus be found by scaling its amplitude to give unit integral, even in the presence of noise with zero mean.

The PSF for each band can then be approximated from the measured LSFs by

$$\tilde{f}(x,y) = LSFx(x)LSFy(y) \tag{2}$$

Obviously, this will only work well for PSFs that can be approximated by such a separable function. As illustrated in Figure 2, it is easy to devise counterexamples where the product of LSFs bears little resemblance to the PSF. It is therefore strongly preferable to align scanning directions with axes of symmetry of the camera under test, such as the along- and across-track directions of a pushbroom scanning camera. Then the PSFs will tend to have shapes that are better represented by the product of LSFs.

An approximation to the PDM (1) can be found from approximate PSFs as

$$\tilde{\varepsilon}_{ij} = \frac{1}{2}\iint_{x,y} \left| \tilde{f}_j(x,y) - \tilde{f}_i(x,y) \right| dxdy \tag{3}$$

Further work would be needed to explore the mathematical range of validity of this approximation. Here we only give some example experimental results below. It is nonetheless clear that the approximate coregistration error estimate (3) has some basic mathematical advantages over one-dimensional methods: Firstly, the full energy of the PSF will tend to

be taken into account, and secondly, the tails of the PSF will tend to be weighted by the area they occupy. On top of this comes the favorable mathematical properties of the PDM [7] as a bound on spectral error.

As defined, the value of the PDM will tend to overestimate the coregistration error due to the contribution from noise in the measurement of LSF, integrated over the scanned area according to (3). Since the scan area needs to extend well outside the PSF to ensure that the full PSF is captured, there would seem to be a risk that the integrated noise could be significant. However, it is important to note that, at least for reflective-domain spectral cameras, photon noise will tend to dominate over readout and dark current noise, particularly so within the main PSF peak. Therefore, the main noise contribution in a measured LSF will tend to come from the peak region. On top of this, it can be observed in (2) that noise in $LSFx$ outside the main peak will tend to be weighted down by the low value of $LSFy$ outside the main peak.

For LSFs measured with a low signal to noise ratio, the noise contribution may of course be significant. A full analysis of noise is omitted here, but we observe that the noise level in our approximated PSFs in Figure 5 below appears to be lower than the reconstruction noise in the full PSF.

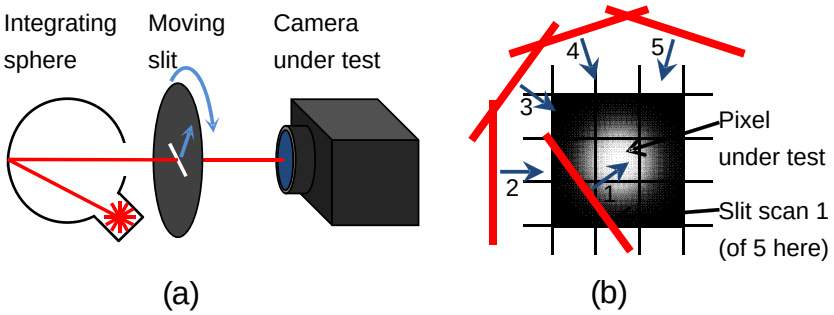

Figure 4. Sketch of the measurement setup. A line source, formed by a slit, is scanned across part of the field of view of a camera under test. The actual PSF is measured by scanning the LSF in many directions, followed by tomographic reconstruction. The approximate PSF is estimated from two orthogonal LSFs taken from the full data set. (b) Illustration of the slit scan pattern in the image plane. The slit scans across the PSF of the pixel under test, in a number of different directions sequentially.

4. EXPERIMENTAL

The results here are based on a new analysis of the data recorded in [8,9]. We therefore already have measurements of the actual two-dimensional PSF for reference.

Briefly, the measurement setup used in [8,9] is illustrated in Figure 4. A line source, formed by a slit much narrower than the nominal pixel width, is scanned across part of the field of view of a camera. The resulting time series recorded from a pixel in a particular band is the line spread function (LSF) for that band. By making linear scans in different directions around the circle, a set of PSF projections is obtained, from which the two-dimensional PSF for each band can be recovered by an inverse Radon transform. With N scan steps across a pixel, and M different scan directions, the transform produces an image of the PSF resolved in $\approx N \times M$ pixels.

The experimental setup is simply a slit mounted on a translation stage, which in turn is mounted on a rotation stage and arranged such that the slit scans across an optical port in the center of rotation. The slit is illuminated from the back by an integrating sphere. Depending on the magnification and pixel size of the camera, the scanned region is typically several pixels across, in order to capture the full extent of the PSF.

Here we show measurement results for two hyperspectral transmission-grating spectrometer cameras. Normally the cameras are used in a line-scanning configuration, but in our measurement the cameras are stationary so that there is no PSF broadening due to scan motion. Both cameras cover the spectral range from 400 to 1000 nm, approximately. The first camera is a SpecIm PFD camera with 1312 pixels across the FOV, dating from 2012, using an OLE23 23 mm objective lens focused at the slit distance of about 1 m. The camera slit width is 30 µm, imaged 1:1 onto detector pixels with 8 µm pitch. Thus, the nominal pixel size is 8×8 µm in the spectrometer slit plane, and the specification implies an IFOV of 1 pixel across and 30/8=3.75 pixels along track. The second camera is a HySpex VNIR-1800 camera with 1800 pixels, dating from 2016, using a 1 m fixed focus lens. This camera has a specified IFOV of 1×2 nominal pixels.

Note that the purpose of this work is not to make a comparative review of the cameras. We point out that the camera found to have better coregistration is also several years newer than the other, and no effort has been made to ensure that the tested units are representative ones.

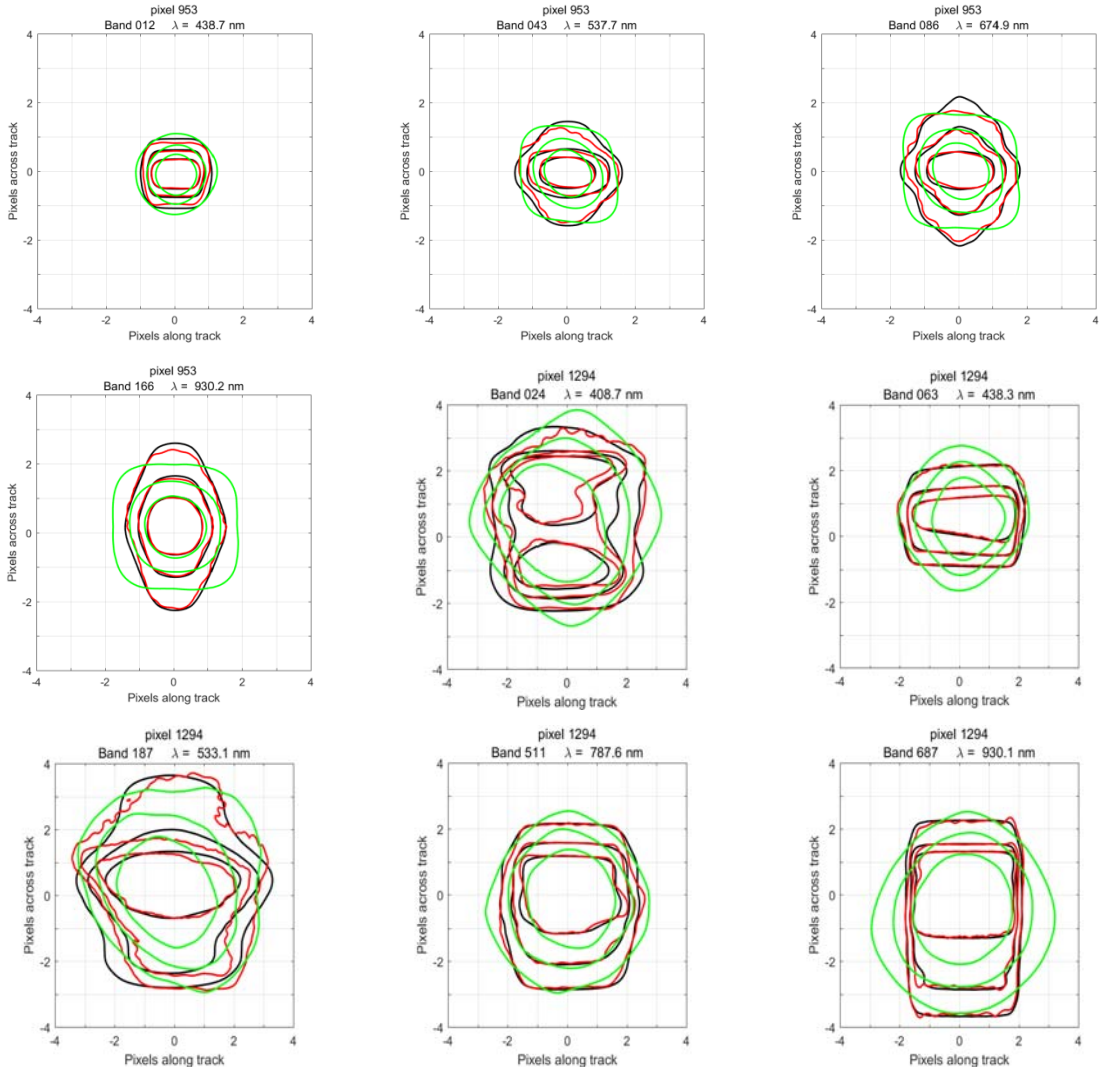

Figure 5. Contour plots of "true" and approximated PSFs recorded with two orthogonal scans for different wavelengths and two different cameras. Contours are drawn for 50, 75 and 90% enclosed energy. Red contours: Full "true" two-dimensional PSF measured by tomographic reconstruction from many LSFs, from [8,9]. Black contours: Approximate PSF reconstructed from LSF scans along and across track. Green contours: PSF reconstructed from "worst case" LSF scans, rotated 45 degrees relative to the along- and across-track directions. The first four plots, marked "pixel 953", are from the center of the field of view of the HySpex camera. The remaining five plots, marked "pixel 1294" are from near the end of the field of view of the older SpecIm camera. The set of plots has been selected to illustrate a variety of PSF shapes.

5. RESULTS

Figure 5 shows a selection of measured PSFs. Each plot shows the PSF measured using the full 2D reconstruction from [8,9] (red) and two approximate PSFs. Black curves show PSFs reconstructed from LSF scans in the along- and across-track directions. Green curves show PSFs recorded in "worst case" directions rotated 45 degrees from the along- and across-track directions.

Consider first the results based on two LSF scans along- and across-track, drawn in black. Comparing to the reference PSF drawn in red, it is immediately clear that the approximation based on two orthogonal scans is able to represent a

variety of different spatial features of the PSF. Recalling that all curves here are based on the same data set, it is also clear that the approximation appears less noisy than the full reconstructed PSFs here. This is reasonable in light of the noise amplification inherent in the reconstruction of the 2D PSF, and also in light of the beneficial noise properties of the approximation discussed in section 3.

The accuracy of the approximate PSF derived from along- and across-track scans clearly benefits from the choice of appropriate scan directions. In the center of the field of view, there is a degree of symmetry which fits well with an assumption of separable PSF. At the edges of the field of view, however, it cannot be taken for granted that the PSF of a pushbroom imaging spectrometer always has a shape that fits with this choice of scan directions. Still, the limited data we have indicates that the approximation works quite well. Some asymmetric features such as "ear" and "banana" components are lost in the separable approximation, but the black contours illustrate that many other features of PSF shape can be well preserved.

Table 1. Values for the mean PDM coregistration error over all band pairs. Values are given for a pixel in the center of the field of view of the HySpex camera, as well as the center and near the end of the field of view of the SpecIm camera. The table gives values derived from the full 2D PSF measurement, as well as for two approximate methods discussed in the text.

	PDM, Full PSF	**Approximate PDM, along/across scan**	**Appxoximate PDM, 45° rotated scan**
HySpex, FOV center	0.20	0.18	0.14
SpecIm, FOV center	0.22	0.20	0.13
SpecIm, FOV end	0.24	0.23	0.19

Table 1 gives values for the mean PDM over all band pairs for a pixel in the HySpex camera and for pixels in the center and end of the FOV of the SpecIm camera. The results show that the PSF approximated from along- and across-track scans underestimates the true value slightly, by about 10%. Such a level of accuracy may still be deemed a sufficiently accurate measure of coregistration performance, particularly in view of the shortcomings of other methods. We have not made any attempts to quantify the effect of tomographic reconstruction noise, but it is worth noting that this noise in the full PSF may lead to some overestimation of the reference PDM value. Therefore the error in the approximate PDF may be smaller than indicated in the table.

When the LSF scan directions are rotated 45 degrees, the detailed PSF shape is lost, as shown by the green contours in Figure 5. This illustrates clearly that the assumption of separable PSF has severe limitations. Nonetheless, it can be observed in Figure 5 that the broadening of the green PSF tends to vary with the broadening of the true PSF. In a sense, coregistration evaluated based on the green PSF approximation reverts to characterizing a combination of peak position and width. It is still possible to calculate a value for the PDM, and the results are shown in the rightmost column of Table 1. The "worst case" scan directions result in a significant underestimation of the PDM error. Still, the results are within a factor 2 of the reference value, and give a fair impression of the differences in coregistration performance. It is likely that in many cases, PSF differences between bands will have a significant component of apparent defocus differences, such as in the PSF measurements on a multispectral camera reported in [10]. In such cases, the approximate PDM method may still give a fair representation of coregistration performance. We note for future work that it may be possible to devise a more robust method for coregistration characterization, based on a few more LSF scans in evenly spaced directions, without resorting to a full 2D reconstruction.

6. CONCLUSIONS

We have presented a method for coregistration characterization based on simple measurement procedures. The proposed method approximates the PSF from two orthogonal LSFs and characterizes coregistration according to the PDM. We have given some example experimental results to illustrate that it appears possible to form good approximations to the PSF in some widely differing experimental cases. Future work could explore the mathematical range of validity of the approximation (2) in relation to the properties of optical systems. However it appears clear that since the approximate PDM method takes the full extent of the PSF into account, it has potential for capturing a larger range of coregistration errors than some other methods, with no added measurement complexity. Due to the favorable properties of the PDM, and the relative ease of measurement, the approximate PDM method appears as an interesting candidate for standardizing coregistration characterization.

REFERENCES

[1] https://standards.ieee.org/project/4001.html
[2] Pantazis Mouroulis, Robert O. Green, "Review of high fidelity imaging spectrometer design for remote sensing," Opt. Eng. 57, 040901 (2018)
[3] Florian Ewald, Tobias Kölling, Andreas Baumgartner, Tobias Zinner, Bernhard Mayer, "Design and characterization of specMACS, a multipurpose hyperspectral cloud and sky imager," Atmos. Meas. Tech. 9, 2015–2042 (2016) (doi:10.5194/amt-9-2015-2016)
[4] Gudrun Høye, Trond Løke, Andrei Fridman, "Method for quantifying image quality in push-broom hyperspectral cameras," Opt. Eng. 54, 053102 (2015)
[5] Torbjørn Skauli, "Quantifying coregistration errors in spectral imaging," Proc. SPIE 8158, 81580A-8 (2011)
[6] G. Lin, R. E. Wolfe, and M. Nishihama, "NPP VIIRS geometric performance status," Proc. SPIE 8153, 81531V-14 (2011)
[7] Torbjørn Skauli, "An upper-bound metric for characterizing spectral and spatial coregistration errors in spectral imaging," Optics Express 20, 918 (2012)
[8] Hans Erling Torkildsen and Torbjørn Skauli, "Full characterization of spatial coregistration errors and spatial resolution in spectral imagers," Opt. Lett. 43, 16 (2018) (doi:10.1364/OL.43.003814)
[9] Hans Erling Torkildsen and Torbjørn Skauli, "Measurement of point spread function for characterization of coregistration and resolution: comparison of two commercial hyperspectral cameras," Proc. SPIE 10644, 106441F (2018)
[10] Hans Erling Torkildsen, Thomas Opsahl, Trym Vegard Haavardsholm, Stéphane Nicolas, Torbjørn Skauli, "Characterization and calibration of a compact 6-band multifunctional camera based on patterned spectral filters in the focal plane", Proc. SPIE 9088 (2014)